Statistical Energy Analysis of a Gearbox with Emphasis on the Bearing Path*

Teik Chin Lim
Structural Dynamics Research Corporation, 2000 Eastman Drive, Milford, Ohio 45150, USA

Rajendra Singh, *Member, INCE*
Department of Mechanical Engineering, The Ohio State University, 206 West 18th Avenue, Columbus, Ohio 43210-1107, USA

*Received: 11 February 1991; revised: 16 July 1991

A generic gearbox containing one spur gear pair is examined using the statistical energy analysis with emphasis on the vibratory energy flow through rolling element bearings. A new analytical procedure has been developed to determine the associated coupling loss factor. Resulting formulation is applied to the NASA helicopter gear noise test facility. Vibro-acoustic predictions at the fundamental gear mesh frequency are found to be in reasonable agreement with measurements even though many simplifying assumptions are made. Such a model can be used for parametric design studies.

Introduction

Vibro-acoustic response of geared systems at low operating speeds can be simulated fairly reliably using deterministic modeling techniques such as lumped parameter method and finite element analysis (FEA).[1-3] However, such classical techniques require extensive computational efforts at high gear mesh frequencies; difficulties may also be encountered in synthesizing or interpreting the vast amount of results.[4-6] Accordingly asymptotic or statistical methods are more suitable at higher response frequencies.[6-10] In particular, the statistical energy analysis (SEA) method has been used by several investigators. For instance, Lyon has shown that the SEA predictions of path transfer functions compare well with measurements of complex structural systems and that the lumped model is inadequate at higher frequencies.[6] Complex gear drives in automotive, helicopter and marine applications have been examined using SEA.[4-6, 11-14] In these investigations, broad band transfer functions and vibratory power flow have been estimated. However, an analytical procedure for the coupling loss factor associated with the rolling element bearing, which is an integral part of the dominant structure-borne path, is yet to be described. To fill this void in the literature, a new SEA model is described in this paper. A generic gearbox is considered and a simple source-path receiver model is constructed and validated through one practical example.

SEA Formulation

Assumptions. A generic gearbox as shown in Fig. 1 is considered. This simple system consists of four identical bearings, two identical casing plates and shafts carrying one spur gear of speed ratio equal to unity. Prime mover and load are not included as it is assumed that they are flexibly coupled to the gearbox. Other assumptions are as follows:

1. Consider steady state linear, time-invariant gear dynamics. The corresponding system vibration and noise (whine) is assumed to be at the mesh frequency ω_h without any sidebands, as excited by the static transmission error e_h.[4,15]
2. During steady-state, both shafts have equal amount of vibratory energy (E_S).
3. Only the structure-borne noise path is assumed since it has been found to be the most dominant.[4,15]
4. Only the shaft bending vibration is coupled to the casing flexural motion through bearings; interactions between torsional and bending modes are ignored.
5. The vibratory energy transfer through each bearing is assumed to be identical.

6. Bearing dimensions are much smaller than the flexural wavelength of the casing plate over the frequency range of interest.
7. Modal densities for the shaft (n_s) and casing plates (n_c) are approximated using ideal simply-supported geometries: $n_s = L_s\,[\rho_s \pi d_s^2/\,(4EI_s\omega^2)]^{0.25}$ and $n_c = (A_c/h_c)\,[3\rho_c(1-\mu^2)/E]^{0.5}$ where ρ is the material density, A_c is the plate surface area, L_s is the shaft length, E is the modulus of elasticity, I_s is the area moment of inertia of the shaft, ω is the bandwidth center frequency, h_c is the plate thickness, d_s is the shaft diameter, μ is the Poisson's ratio, and the subscripts s and c denote shaft and casing plate, respectively.[6]
8. The gearbox is mounted on rigid mounts.
9. The casing plate motion is spatially uniform.
10. The dissipation mechanism for this system includes structural damping, acoustic energy radiated from the casing plate and the torsional vibratory energy transmitted to the load or prime mover.
11. Casing plates are the primary radiators of sound in an environment given by room constant $R(\omega)$.

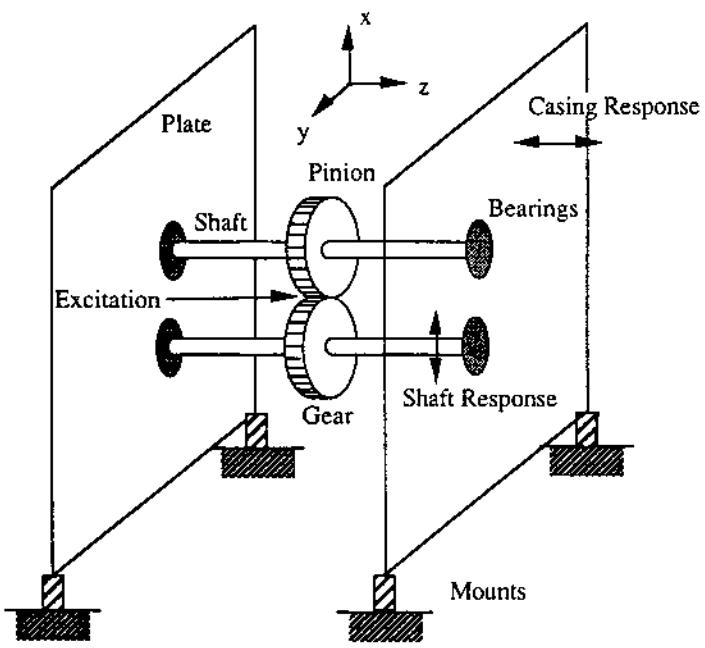

Figure 1. A generic geared rotor system with casing and mounts

Theory. Application of the SEA principle results in two subsystems, one internal consisting of gears, shafts and bearings, and one external consisting of casing plates and mounts, as shown in Fig. 2. The vibratory energy transfer from the internal subsystem to the external subsystem in this case is the algebraic sum of the energy transmitted through four bearing connections, similar to the single vibratory energy path concept. Since the general solution methodology for such subsystems is well known, the mean-square velocity levels of the gears-shafts-bearings subsystem $\langle V_s^2 \rangle$ and casing-mount subsystem $\langle V_c^2 \rangle$ are[6]:

$$\langle V_s^2 \rangle\,(\omega) = \frac{\Pi_f(\eta_{cT} + 4\eta_{cs})}{m_s\omega(\eta_s\eta_{cT} + 4\eta_{cT}\eta_{sc} + 4\eta_s\eta_{cs})}\ ; \qquad (1a)$$

$$\langle V_c^2 \rangle\,(\omega) = \frac{4\Pi_f\eta_{sc}}{m_c\omega(\eta_s\eta_{cT} + 4\eta_{cT}\eta_{sc} + 4\eta_s\eta_{cs})} \qquad (1b)$$

where ω is the bandwidth center frequency, η_{sc} is the coupling loss factor, $\eta_{cs} = \eta_{sc}n_s/n_c$, Π_f is the power input at the gear mesh source, η_s is the internal subsystem dissipation loss factor, m_c is the casing mass and m_s is the internal subsystem total mass. Additionally, η_{cT} is the total dissipation loss factor for the casing plate due to structural damping and acoustic energy radiated, which will be formulated later.

The frequency-averaged formulation for η_{sc} is based on the deterministic solution of the shaft-bearing boundary value problem assuming rigid casing plates. We have already proposed it for a single shaft-bearing, single-plate system in Refs. 16 and 17. This formulation is extended here further to examine the gearbox of Fig. 1. Note that η_{sc} is given in terms of point moment impedances for the shaft Z_s and flat plate Z_c, and of flexural rigidity for the shaft EI_s and shaft length L_s in the following:

$$\eta_{sc}(\omega) = \frac{4EI_s}{\omega L_s} Re\left\{\frac{1}{Z_c}\right\}\left|\frac{Z_c}{Z_c + Z_s}\right|^2 . \qquad (2)$$

For an infinite steel plate of thickness h_c with circular input patch of diameter d_s, the point moment impedance Z_c is given by[18]

$$Z_c(\omega) = \frac{4Eh_c^3}{3\omega(1-\mu^2)}\left\{1 - \frac{4i}{\pi} ln\left(\frac{9}{20}k_c d_s\right)\right\}^{-1}\ ;\ k_c d_s << 1\ . \qquad (3)$$

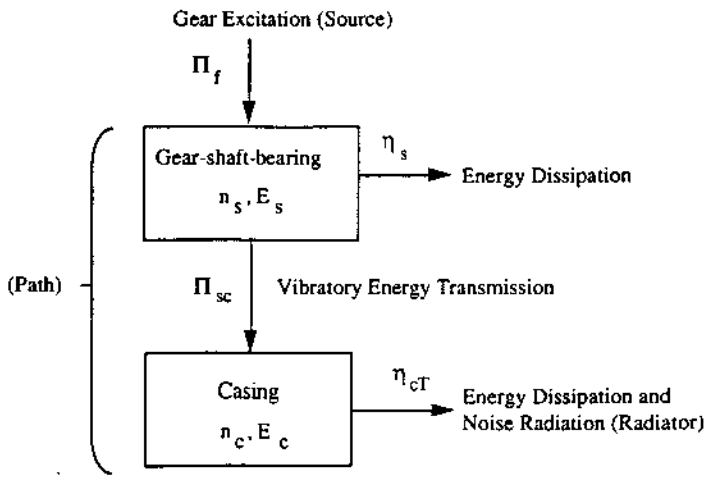

Figure 2. An approximate SEA model of a geared rotor system

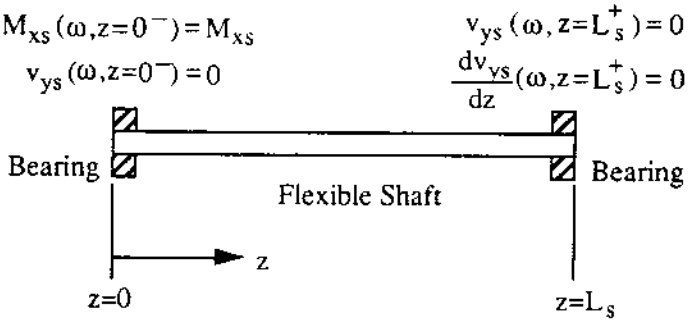

Figure 3. Boundary conditions for a finite shaft-bearing system

The driving point impedance of the shaft Z_s used in Eq. (2) is derived next with the boundary conditions as shown in Fig. 3. At the left bearing end of the shaft ($z=0^-$), $v_{ys}(\omega,z=0^-)=0$, and $M_{xs}(\omega,z=0^-)=M_{xs}$. In the frequency domain, using the definition of bearing force vector $\{f(\omega)\}_b=[K]_{bm}\{v(\omega)\}_b/i\omega$ in terms of the velocity vector $\{v(\omega)\}_b$ and the bearing stiffness matrix $[K]_{bm}$, these conditions are equivalent to $M_{xs}(\omega,z=0^+)=M_{xs}$, and $F_{ys}(\omega,0^+)=(k_{by\theta_x}/k_{b\theta_x\theta_x})M_{xs}+v_{ys}(\omega,0^+)\ [(k_{by\theta_x}/k_{b\theta_x\theta_x})^2k_{b\theta_x\theta_x}-k_{byy}]/(i\omega)$. Explicit expressions for the entries of $[K]_{bm}$ are given in Ref. [19]. Similarly, the other bearing end of the shaft at $z=L_s^+$ with zero translational and angular velocities is described at $z=L_s^-$ as

$$M_{xs}(\omega,z=L_s)=-\left[k_{b\theta_x\theta_x}\frac{dv_{ys}}{dz}(\omega,L_s^-)+k_{by\theta_x}v_{ys}(\omega,L_s^-)\right]/(i\omega) \quad ; (4a)$$

$$F_{ys}(\omega,z=L_s)=-\left[k_{by\theta_x}\frac{dv_{ys}}{dz}(\omega,L_s^-)+K_{byy}v_{ys}(\omega,L_s^-)\right]/(i\omega) \quad . (4b)$$

The governing equations for the bending motion of a shaft and the assumed solution are[15]:

$$M_{xs}=-\frac{EI_s}{i\omega}\frac{d^2v_{ys}}{dz^2} \quad ; \quad F_{ys}=\frac{EI_s}{i\omega}\frac{d^3v_{ys}}{dz^3} \qquad (5a,b)$$

$$v_{ys}(t,z)=\{b_1e^{-jk_sz}+b_2e^{jk_sz}+b_3e^{-k_sz}+b_4e^{k_sz}\} \quad . \qquad (6)$$

The modified boundary conditions can then be evaluated to formulate an algebraic problem of the type given by

$$[B]\{b\}=M_{ys}\{k_{by\theta_x}/k_{b\theta_x\theta_x},\ i\omega/(EIk_s^2),0,0\}^T \quad , \qquad (7)$$

where the nonzero elements of the coefficient matrix $[B]$ are

$$B_{11}=\frac{1}{\omega}\left\{EIk_s^3-ik_{byy}+\frac{ik_{by\theta_x}^2}{k_{b\theta_x\theta_x}}\right\} \ ; \ B_{12}=\frac{1}{\omega}\left\{-EIk_s^3-ik_{byy}+\frac{ik_{by\theta_x}^2}{k_{b\theta_x\theta_x}}\right\} \ ;$$

$$B_{13}=\frac{i}{\omega}\left\{EIk_s^3-k_{byy}+\frac{k_{by\theta_x}^2}{k_{b\theta_x\theta_x}}\right\} \ ; \ B_{14}=\frac{i}{\omega}\left\{-EIk_s^3-k_{byy}+\frac{k_{by\theta_x}^2}{k_{b\theta_x\theta_x}}\right\} \ ;$$

$$B_{21}=B_{22}=-B_{23}=-B_{24}=1 \ ;$$

$$B_{31}=(-jk_sk_{b\theta_x\theta_x}+k_{by\theta_x}+EIk_s^2)\,e^{-ik_sL_s} \ ;$$

$$B_{32}=(jk_sk_{b\theta_x\theta_x}+k_{by\theta_x}+EIk_s^2)e^{ik_sL_s} \ ;$$

$$B_{33}=(-k_sk_{b\theta_x\theta_x}+k_{by\theta_x}-EIk_s^2)\,e^{-k_sL_s} \ ;$$

$$B_{34}=(k_sk_{b\theta_x\theta_x}+k_{by\theta_x}-EIk_s^2)\,e^{k_sL_s} \ ;$$

$$B_{41}=(ik_sk_{by\theta_x}-k_{byy}-iEIk_s^3)\,e^{-ik_sL_s} \ ;$$

$$B_{42}=(-ik_sk_{by\theta_x}-k_{byy}+iEIk_s^3)\,e^{ik_sL_s} \ ;$$

$$B_{43}=(k_sk_{by\theta_x}-k_{byy}+EIk_s^3)e^{-k_sL_s} \ ;$$

$$B_{44}=(-k_sk_{by\theta_x}-k_{byy}-EIk_s^3)\,e^{k_sL_s} \quad . \qquad (8)$$

By definition, the bearing-shaft point moment impedance Z_s is then given by

$$Z_s(\omega)=\frac{M_{xs}(\omega,0)}{\frac{dv_{ys}}{dz}(\omega,0^-)}=\frac{k_{b\theta_x\theta_x}}{i\omega+\frac{k_{by\theta_x}v_{ys}(\omega,0^+)+k_{b\theta_x\theta_x}\frac{dv_{ys}}{dz}(\omega,0^+)}{M_{xs}}} \quad . \qquad (9)$$

Vibro-Acoustic Response. Input power Π_f by the gear mesh elastic force $F_h=k_he_he^{i\omega_ht}$ is given by $\Pi_f(\omega_h)=0.5(k_he_h)^2Re\{1/Z_f(\omega_h)\}$ where k_h is the gear mesh stiffness. Assuming the excitation is far removed from the boundaries, the driving point impedance is $Z_f=2\rho_sA_sc_s(1+i)+i\omega m_g$ where ρ_s, A_s and c_s are the density, cross sectional area and wave speed of the shaft respectively, and m_g is the gear mass.[18] Note that Π_f can be increased by a higher amplitude of gear transmission error e_h and a lower $Re\{1/Z_f(\omega_h)\}$. For a specific example such as the NASA gearbox considered here, these parameters are generally known; hence Π_f is specified. The total dissipation loss factor η_{cT} for the casing of area A_c, mass m_c and radiation efficiency σ_c is

$$\eta_{cT}(\omega)=\eta_c+\frac{z_oA_c\sigma_c(\omega)}{\omega\, m_c} \quad , \qquad (10)$$

where z_o is medium characteristic impedance and η_c is due to casing plates structural damping. Here, two σ_c models are used: (a) $\sigma_{c1}=1.0$ for an ideal radiator as seen for many practical gearboxes over the frequency range of interest, and (b) σ_{c2} for a simply-supported rectangular plate.[15,20] For the internal subsystem, the dissipation loss factor is assumed to be $\eta_s=\gamma\eta_c$ where $\gamma\geq1$ due to additional losses at the gears, bearings and load.

Sound power level L_W (dB *re* W_{ref} = 1*pW*) radiated from the casing is computed using

$$L_W(\omega) = 10 \log_{10}\left\{\frac{W(\omega)}{W_{ref}}\right\} \; ; \; W(\omega) = \sigma_r A_c \langle V_c^2(\omega)\rangle \sigma_c(\omega) \quad . \quad (11a,b)$$

Assuming a source directivity Q(w) associated with the gearbox mounting condition, the sound pressure level L_p (dB re 20μPa) in the far field, given room constant $R(\omega) = \bar{\alpha}\, S/(1-\bar{\alpha})$, at distance r from the casing, is as follows where $\bar{\alpha}(\omega)$ is the average absorption coefficient and S is the room surface area:

$$L_p(\omega) = L_W(\omega) + 10 \log_{10}\left\{\frac{Q(\omega)}{4\pi r^2} + \frac{4}{R(\omega)}\right\} . \quad (12)$$

Application Example

NASA Gearbox. The SEA formulation is verified by comparing results with vibro-acoustic responses measured on the NASA Lewis Research Center helicopter gearbox. A schematic of the gear noise test facility is given in Fig. 4 which shows the locations for the casing vibration measurements and unweighted L_p at $r \simeq 0.38$ m, directly above the top casing plate. An approximate configuration and nominal dimensions of the high precision gearbox are shown in Fig. 5. Rigid mount feet attach the four corners of the bottom casing plate to a massive foundation. High precision gear and pinion which are identical with 0.006m facewidth and 0.089m diameter are installed. Four axially preloaded high precision deep groove ball bearings are used to support 0.03m diameter shafts of length 0.254m on the casing. The input and output shafts are only coupled torsionally to the rest of the test facility through flexible couplings. The geared system is driven by a 149kW d.c. motor, over an operational speed range of 1000-5990 rpm. The corresponding gear mesh frequency ω_h range is 467-2777 Hz. From the gear tooth profile and geometry, the gear static transmission error at ω_h is computed as: $e_h(t) \simeq 3.5 \sin(\omega_h t)$, μm.[21] It may be noted that even though the practical example case presented here does not meet all of the requirements for SEA, we still apply our theory in order to develop an order of magnitude prediction model.

Results

The NASA gearbox is run at each speed of interest and sound pressure level L_p and spatially averaged mean square acceleration level ($\omega^2 < V_c^2 >$) spectra are acquired by processing the measured data only at corresponding ω_h; casing motions were measured for a limited range of ω_h. Analogous predictions using the proposed theory are based on the calculations of η_{sc} which is reported in Table 1. Note that the bearing preload is taken to be given by the equivalent mean axial deformation $\delta_z \simeq 0.04$mm. Note that it is difficult to maintain and even to measure accurately the preload required for each test. Accordingly, there is some uncertainty associated with η_{sc} values.

Predicted and measured L_p spectra on 1/3-octave basis are compared in Fig. 6(a) for γ=10, $\sigma_c = \sigma_{c2}$ and δ_z=0.04mm. The second term in Eq. (12) is dominated by $Q/(4\pi r^2)$ since $4/R \ll Q/(4\pi r^2)$ for the NASA test facility due to $\bar{\alpha} \simeq 1.0$ and room surface area S being very large. Predictions are found to be within ±10dB of the measured values for typical lightly damped structural dissipation loss factor $0.004 \le \eta_c \le 0.04$. Figure 6(b) shows the comparison of casing acceleration between theory and experiment. The experimental curve represents the averaged value of the measurements made at three casing plate locations (top plate, side plate with bearings and side plate without bearings). Again, predicted acceleration spectra, which are similar to those found for the sound pressure level, are in reasonable agreement with the measured spectrum given typical values of η_c and γ. In general, we observe that the response level decreases with increasing η_c. Also, comparisons suggest that η_c in this system may be frequency dependent.

Next we vary γ but keep η_c=0.02 in Fig. 7. Comparison between theory and measurements also indicates that γ=10 is the best fit for the experimental data, especially at the higher frequencies. This result is reasonable since the dissipation loss factor η_s of subsystem consisting of gears, bearings and load is typically much higher than the internal loss factor η_c for a lightly damped casing. Here, radiation efficiency σ_{c1} have been used with δ_z=0.04mm. Now we investigate the effect of casing plate radiation efficiency σ_c on L_p. Figure 8 compares σ_{c1} and σ_{c2}. Based on the comparison with experiment it seems that the radiation efficiency of the NASA gearbox is better modeled with σ_{c1} although the measured L_p curve is mostly between σ_{c1} and σ_{c2} curves. Differences between σ_{c1} and σ_{c2} are significant at lower frequencies, but the variation never exceeds 10dB over the entire frequency range of interest. This result is consistent with other experimental observations of typical gearbox systems having nearly unity radiation efficiencies.[15] It may be noted that since the acoustic energy radiated $W(\omega)$ is significantly smaller than the energy dissipated by the system, virtually no change is found in the predicted casing acceleration spectra by varying σ_c.

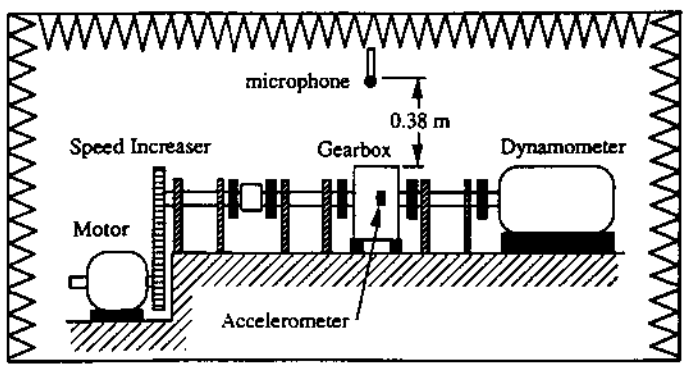

Figure 4. Schematic of the NASA Lewis Research Center spur gear noise test facility

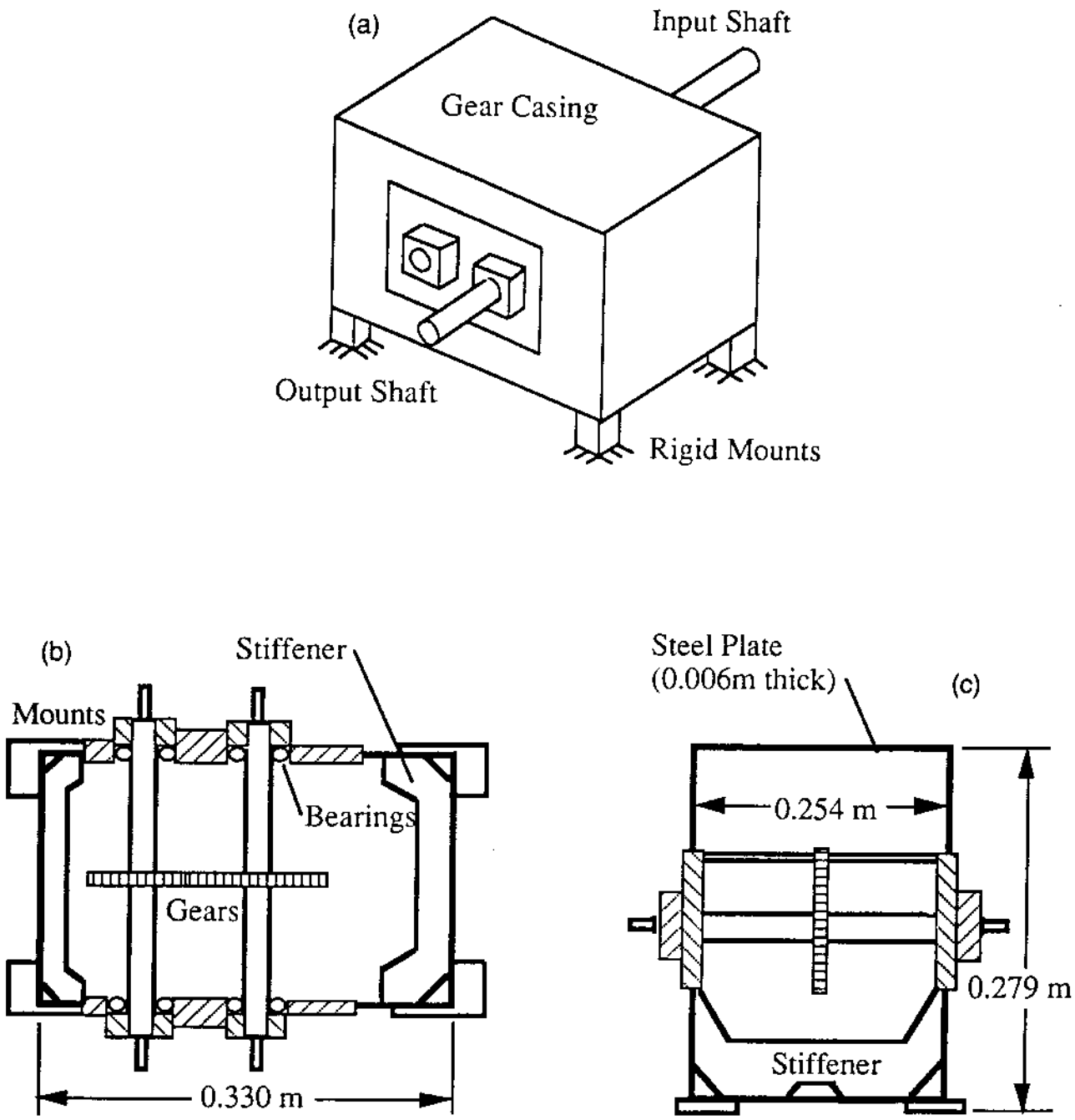

Figure 5. Schematic of the NASA gearbox.
(a) external view
(b) internal plan view
(c) internal elevation view

TABLE 1
COUPLING LOSS FACTOR η_{ac} FOR THE NASA GEARBOX

One-third Octave Band Center Frequency (Hz)	Coupling Loss Factor η_{ac}
500	1.88×10^{-4}
630	1.96×10^{-4}
800	2.09×10^{-4}
1000	2.77×10^{-4}
1250	2.60×10^{-4}
1600	3.37×10^{-4}
2000	5.87×10^{-4}
2500	231×10^{-4}
3150	0.0291×10^{-4}
4000	0.421×10^{-4}

Bearing parameters: deep groove ball bearing type, number of rolling elements=12, radial clearance=0.005mm, pitch diameter=38.5mm, and unloaded distance between inner and outer raceway groove curvature centers=0.0625mm.

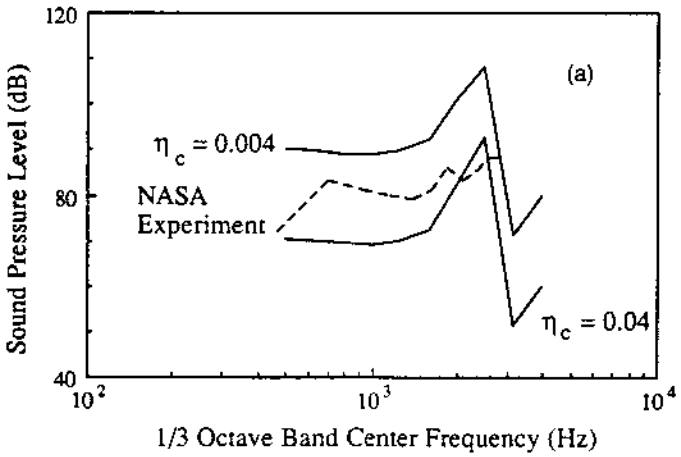

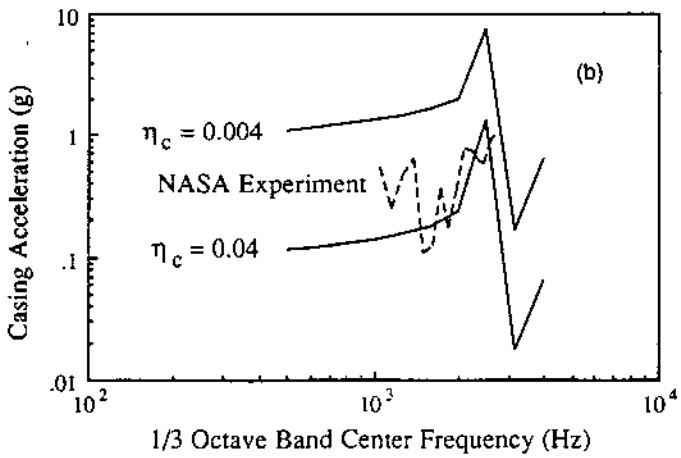

Figure 6. Comparison between theory and experiment (γ=10, Q=2, $\sigma_c = \sigma_{c2}$, δ_z= 0.04mm).
(a) sound pressure level L_p
(b) spatially averaged casing acceleration

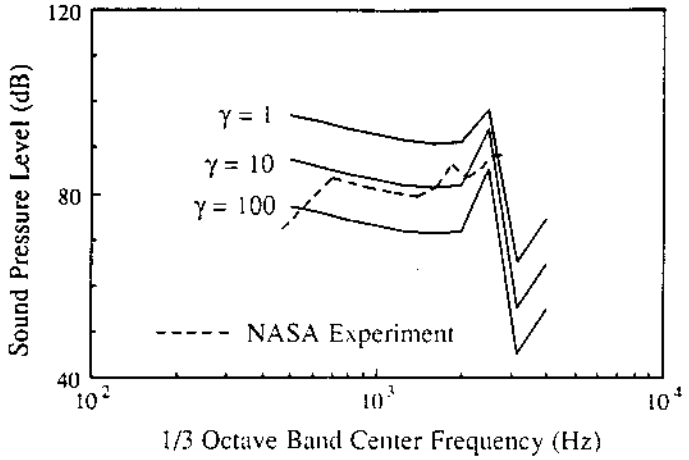

Figure 7. Effect of $\gamma = \eta_s/\eta_c$ on predicted L_p (η_c=0.02, Q=2, $\sigma_c = \sigma_{c1}$, δ_z=0.04mm)

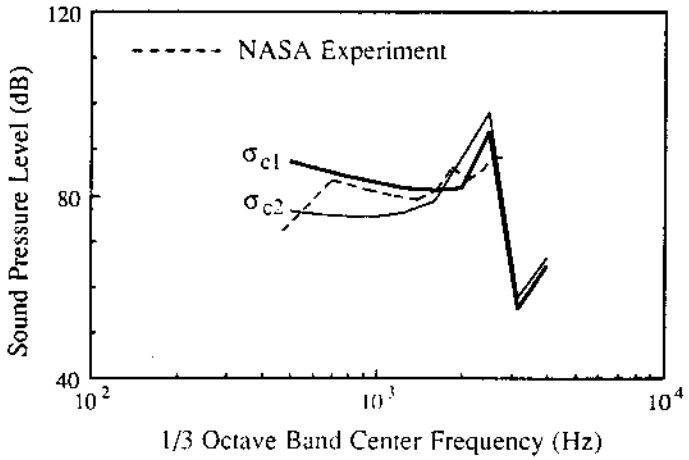

Figure 8. Sound pressure level prediction with two σ_c formulations: σ_{c1} = 1.0 (ideal radiator) and σ_{c2} for simply-supported plate (γ=10, Q=2, η_c=0.02, δ_z=0.04mm)

Conclusion

A simplified SEA model has been developed for a generic gearbox. This model includes a theoretical coupling loss factor associated with the transmission of vibratory energy through the dominant path, i.e., rolling element bearings. The NASA Lewis Research Center gearbox is used as an example. Experimental results are in reasonable agreement with the proposed SEA model even though many simplifying assumptions are involved; discrepancies are also due to the fact that there are uncertainties associated with the estimation of system parameters. Accordingly the proposed formulation should be considered as an order of magnitude model. Further investigation is needed

to resolve several research issues such as the interaction between shaft torsional and bending modes. The model presented here could also be expanded to examine energy sharing between various subsystems in a multi-mesh geared system.

Acknowledgment

We wish to thank the NASA Lewis Research Center for supporting this research at the Ohio State University, and James J. Zakrajsek and Fred B. Oswald for providing the test data.

References

1. A Kahraman, H.N. Ozguven, D.R. Houser and J.J. Zakrajsek, "Dynamic Analysis of Geared Rotors by Finite Elements," *Proceedings of the International Power Transmission and Gearing Conference* (American Society of Mechanical Engineers, New York, 1989), pp. 375-382.
2. S.V. Neriya and T.S. Sankar, "Coupled Torsional-Flexural Vibration of a Geared Shaft System Using Finite Element Method," *The Shock and Vibration Bulletin*, **55**(3), 13-25 (1985).
3. D. Astridge and M. Salzer, "Gearbox Dynamics-Modeling of a Spiral Bevel Gearbox," Paper 50 (Third European Rotorcraft and Power Lift Aircraft Forum, France, 1977).
4. T.C. Lim and R. Singh, "A Review of Gear Housing Dynamics and Acoustic Literature," NASA Contractor Report 185148, (October 1989).
5. W.B. Rockwood, L.K.H. Lu, P. Warner and R.G. DeJong, "Statistical Energy Analysis Applied to Structureborne Noise in Marine Structures," *Statistical Energy Analysis*, K.H. Hsu, D.J. Nefske and A. Akay, Eds. (American Society of Mechanical Engineers, New York, 1987), pp. 73-79.
6. R.H. Lyon, *Statistical Energy Analysis of Dynamical Systems* (The MIT Press, Cambridge, 1975).
7. J. Woodhouse, "An Introduction to Statistical Energy Analysis of Structural Vibration," *Applied Acoustics*, **14**, 455-469 (1981).
8. E.H. Dowell and Y. Kubota, "Asymptotic Modal Analysis and Statistical Energy Analysis of Dynamical Systems," *Journal of Applied Mechanics*, **52**, 949-957 (1985).
9. Y. Kubota, H.D. Dionne and E.H. Dowell, "Asymptotic Modal Analysis and Statistical Energy Analysis of an Acoustic Cavity," *ASME Journal of Vibration, Acoustics, Stress, and Reliability in Design*, **110**, 371-376 (1988).
10. E. Skudrzyk, "The Mean-value Method of Predicting the Dynamic Response of Complex Vibrators," *Journal of the Acoustical Society of America*, **67**(4), 1105-1135 (1980).
11. R.H. Lyon, *Machinery Noise and Diagnostics* (Butterworth Publishers, Stoneham, Massachusetts, 1987).
12. J.S. Pollard, "Helicopter Gearcase Structure-Borne Noise Studies Using Statistical Energy Analysis Modelling," *Gearbox Noise and Vibration* (Institution of Mechanical Engineers, London, 1990), pp. 69-81.
13. N. Lalor, J.D. Dixon and G.J. Stimpson, "Source Identification of Automotive Gearbox," *Gearbox Noise and Vibration* (Institution of Mechanical Engineers, London, 1990), pp. 83-96.
14. L.K.H. Lu, W.B. Rockwood, P.C. Warner and R.G. DeJong, "An Integrated Gear System Dynamics Analysis Over a Broad Frequency Range," *The Shock and Vibration Bulletin*, **55**(3), 1-11 (1985).
15. R. Singh, "The Ohio State University Gear Noise Short Course," Columbus (1989).
16. T.C. Lim and R. Singh, "Coupling Loss Factor of a Shaft-Bearing-Plate System," *Proceedings of the International Conference on Noise Control Engineering*, H.G. Jonasson, Ed. (Institute of Noise Control Engineering, Poughkeepsie, New York, 1990), Vol. II, pp. 957-960.
17. T.C. Lim and R. Singh, "Vibration Transmission Through Rolling Element Bearings, Part IV: Statistical Energy Analysis," *Journal of Sound and Vibration*, in press (1991).
18. L. Cremer, M. Heckl and E.E. Ungar, *Structure-Borne Sound* (Springer-Verlag, Berlin, 1973).
19. T.C. Lim and R. Singh, "Vibration Transmission Through Rolling Element Bearings, Part I: Bearing Stiffness Formulation," *Journal of Sound and Vibration*, **139**(2), 179-199 (1990).
20. G. Maidanik, "Response of Ribbed Panels to Reverberant Acoustic Fields," *Journal of the Acoustical Society of America*, **34**(6), 809-826 (1962).
21. A. Kahraman, "Non-Linear Dynamic Analysis of Geared Systems," Ph.D. Dissertation, The Ohio State University, (1990).